**ROYAL
AERONAUTICAL
SOCIETY**

REGULAR PAPER

Fretting wear behaviour in 6061-T6 aluminium alloy

V. Erturun[1] and D. Odabas[2]

[1]Department of Airframes and Powerplants, Faculty of Aeronautics and Astronautics, Erciyes University, 38039, Kayseri, Türkiye and [2]Department of Mechanical Engineering, Faculty of Engineering, Erciyes University, 38039, Kayseri, Türkiye
Corresponding author: V. Erturun; Email: erturun@erciyes.edu.tr

Abstract
In this study, fretting wear in riveted lap joints of aluminium alloy plates was investigated. For the fretting test, 6061-T6 aluminium alloy plates, which are widely used in aircraft construction, and blind rivets were used. Experiments were carried out using a computer controlled Instron testing machine. Fretting surface roughness, microhardness was investigated by metallographic techniques and scanning electron microscopy.

Tensile load cycles in the riveted lap joint were found to cause damage to all surfaces. Two contact surfaces where friction occurs were investigated. The contact surface of the lower plate with the upper plate, and the contact surface of the lower plate with the rivet head. As load and cycles increased, fretting scars and surface roughness increased.

Consequently, it has been determined that fretting damages occur between the contact surface of the plates and between the plate and the rivet contact surface.

1.0 Introduction

The use of carbon fibre reinforced polymer and aluminium alloy has increased rapidly for the aerospace manufacturing industry due to its excellent mechanical properties in lightness and durability and assembling structural components is essential for aircraft assembly [1, 2].

The difficulties encountered in understanding fretting and evaluating its results are of importance. It is considered that there is enough information to put the whole issue on a rational basis, but more research is needed to eliminate some of the uncertainties that still remain [3].

Fatigue of transport airframes due to pressurisation is an important problem that aircraft manufacturers and users have to overcome, for reasons such as ensuring the safety of the fuselage, its useful life and formulating adequate inspection procedures. The fatigue problem of lap joints has been significantly expanded to extend aircraft life [4].

The results of the finite element study of the bolted lap joint showed that when subjected to a longitudinal tensile load, the higher clamping force can significantly reduce the magnitude of the tensile stress at the hole edge as well as the bearing stress in the joint [5]. The only certainty is that the prediction is unlikely to be completely correct. This also applies to studying the future of airframe materials [6]. Analysis of cracks obtained in fretting fatigue tests was performed when there was a small oscillating contact. For this contact geometry and testing, a numerical model was developed. The results obtained were compared with the actual crack result measurements [7].

Considering research into future riveting applications, interfacial friction can cause fretting and potentially lead to corrosion problems. In a riveted lap joint, bending stress at the lap edge can cause stress concentration [8]. He used the Finite Element method to examine fretting fatigue and crack initiation for aluminium alloy aircraft components. The results show that the external load has a significant effect on the crack initiation location of the specimen [9].

Table 1. *Composition of AA 6061-T6 alloys*

Alloy	CU	Mg	Cr	Si	Temper
6,061	0.25	1.00	0.25	0.60	T6: Solution heat treated and artificially aged

When the effect of fretting on the fatigue performance of microstructures for different titanium alloys was examined, it was understood that the strength fatigue of Ti6Al4V titanium was lower than that of Ti1023 titanium. But the fretting fatigue of Ti6Al4V titanium is higher under each contact stress. The wear mechanism of the two titanium alloys is different, Ti1023 titanium alloy is more susceptible to fretting wear [10]. The effect of relative slip on the fretting fatigue behaviour of 2014 aluminium alloy with T4 and T6 aged conditions in contact with AISI 1,045 steel shows that T6 is more effective at improving fretting fatigue life compared to natural temper T4 [11]. It was concluded that Ni/nano-TiC composite coatings exhibit low-fretting coefficient, high-fretting wear resistance and high nanohardness in wet conditions compared to pure Ni coatings [12]. Duplex and composite coatings are better than single-layer coatings for extending service life, reducing maintenance and replacement costs while improving the tribological properties of a wide variety of engineering materials in the thermal spray technique [13].

Residues from mechanical wear are easily oxidised by the high temperatures created by friction between surfaces. Depending on the metals involved, the third body of residue can either be acid as a lubricant, which reduces the coefficient of friction between the two surfaces, or it can act as an abrasive, exacerbating wear damage. Residual is compressed into surfaces, often causing depressions and grooves. Surface imperfections create stress amplifiers that accelerate fatigue. Surface defects create stress risers that accelerate fatigue. When friction occurs between metals of different hardness, the softer metal deforms the most [14].

The useful life of most tribological joints is related to wear or deterioration of the friction components due to fretting due to the oscillation of friction surfaces. Such oscillations are caused by vibrations, reciprocating motion, periodic torsion or bending of the mating component, etc. why could it be. The slip between the connecting surfaces is an indispensable condition for the formation of friction. Fretting also tangibly reduces surface quality and produces increased surface roughness, micropits [15].

2.0 Experimental procedures

2.1. Materials and specimens

Material specifications are listed in Table 1. Aluminium alloy sheet was supplied by Alcan International. The sheet was also coated with a wax-based lubricant whose concentration was below 1%. High-quality 6061-T6 aluminium alloys are primarily used in aircraft with their high strength, flexibility and corrosion resistance.

Sheets have recently found widespread use as large, small and kit aircraft building materials. Sheets have recently found widespread use as large, small and kit aircraft building materials. Additionally, almost all other aircraft types use sheet metal to some degree [16].

Sheet-metal aircraft structure has become an alternative to fabric-covered tubular steel fuselage due to its many advantages. Metal construction is more efficient as it does not need both a separate coating to provide the aerodynamic shape and a frame for structural strength. Also, sheet metal is not as delicate as cloth and is not damaged by moisture and sunlight. The aluminium alloy construction is very durable yet lighter. Due to the physical properties of metal parts and fasteners, the metal aircraft will carry the required loads and resist stress, providing superior strength and durability while reducing weight, thus increasing performance.

The density of AA 6,061 alloy at $20\,^{\circ}$C is 2.70 gr/cm^3. The usage temperature as coated and uncoated alloy is 260–510 $^{\circ}$C [17]. Mechanical properties of AA 6,061 T6 alloy are given in Table 2.

Blind rivets can be adjusted very easily by accessing from one side. The hand rivet gun is kept perpendicular to the material while the blind rivet is being pulled, and the rivet gun is pressed down while the

Table 2. *Mechanical properties of AA 6,061 T6 alloy*

Alloy (AA)	Temper	Tensile Strength (Kg/mm²)	Yield Strength (Kg/mm²)
6,061	T6	31	28

rivet is tightened. Blind rivets made from quality alloys have shear strength tested in batches before shipping. These rivets are corrosion resistant and lock after the handle is set. Also, very different lengths are not necessary for different diameters or thicknesses. It is mentioned as 1/8 rivet in the assembly information. Design shear strength is given as 130 lbs [16].

Blind rivets are widely used, which contribute to the simple joining of the metal structure. When pulling blind rivets, it is almost silent compared to the slamming sound of a pneumatic hammer and is well suited for home projects. Also, the process is fast and seamless, thanks to the inherent simplicity of blind rivets. For metal planes it's totally simple, no countersunk required for straight riveting to outer skins. While accounting for the hundreds of construction hours required to achieve perfectly smooth exteriors, it has a negligible impact on performance. Another advantage of blind rivets is their long grip lengths; this means that the same rivet size can be used to hold a wide variety of material thicknesses, eliminating the need for a large inventory of rivets of different lengths. While the cost per unit is higher for blind rivets, it provides many benefits to home builders and provides the necessary strength, durability and ease of construction, making many modern metal kits very popular on aircraft. Nothing looks faster than pop-riveted aluminium. From race cars to airplanes, blind rivets are the fastener of choice for joining sheet metals [18].

2.2 Riveted joint

Plates of 100 mm length and 50 mm width were prepared from AA 6061-T6 aluminium alloy plates. The boards were clamped on top of each other with a 20 mm overlap. A double-riveted joint sample was prepared with a distance of 30 mm between two rivets. This value has been determined by considering the dimensions given in the aircraft's manufacturing books.

When multiple rivets are to be made, Clecos are attached to other holes to prevent off-centre. The riveting process of the aluminium plates was carried out with an air-drawn rivet gun.

The macroscopic cross-sectional view of the rivet joint after riveting is shown in Fig. 1. The cross-sectional view of the joint area is taken perpendicular to the load to be applied. In this study, two interfaces A and B, which are exposed to friction, were investigated in the blind rivet joint indicated in the cross-sectional image. Surface A of the bottom plate contacting the top plate, surface B of the bottom plate contacting the rivet head [19].

2.3. Fretting experiments

Frettin experiments were tested on a computer-controlled servohydraulic universal Instron Testing machine. A cyclic tension-tension load with a sinusoidal waveform at a frequency of 20 Hz is applied in the main cyclic load control. Attention has been paid to ensure that the load coming to the joint is homogeneously distributed. In the fretting experiments, three different loads of 240, 480 and 960 N were applied in 2×10^4 and 6×10^4 cycles. Fatigue life has been determined as 866,920 cycles. Experimental data were entered into the system with the Max package program.

In the fretting tests, the rivet joint was separated, and wear traces were detected on the mating surfaces of the plates and on the contact surfaces between the plate and the rivet by scanning electron microscopy (SEM). The roughness values of the surfaces indicated by A and B belonging to the joint were measured with the Mitutoyo Surftest 201 device. Microhardness values were measured with the mhp 160 model microhardness head that can be mounted on a Janevert brand metal microscope.
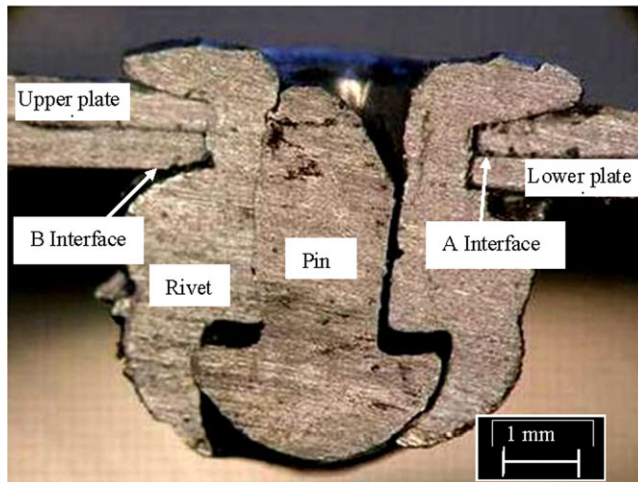
Figure 1. *Cross-section of unloaded A4 blind rivet joint.*

3.0 Result and discussion

3.1 Investigation of fretting damage

In this examination, it was determined that there was wear damage on the contact surfaces of A and B in the blind rivet connection (Fig. 1).

3.1.3 Fretting at the contact surface of the lower plate with the upper plate

Effect of Load on Fretting Damage

Fretting zones formed on the A contact surface was observed for 2×10^4 loading cycles and loads of 480 N. Here, very little blackness has occurred next to the scars of friction and fretting that occurred during riveting on the edge of the hole. The reason why these scars are wide is the compression of the plates by the rivet head, since the plate surfaces are wider and flatter than the rivet head due to compression, they come into contact with each other in a wider area. It is seen in the form of blackness in contact areas.

Fretting zones were detected at 480 N at 4×10^4 cycles. Here, the fretting scars are seen more clearly as the cycle increases. Events occurred at the interface between the upper plate and the lower plate. For the fretting zones formed at 480 N in 6×10^4 cycles, the fretting scars are more prominent as the cycle increases.

3.1.4. Fretting at the contact surface of the lower plate with the rivet making head

Effect of Load on Fretting Damage

The fretting zones formed on the B contact surface at 480 N in the joints in 6×10^4 cycles are shown in Fig. 2. The figure shows three body fretting zones at the edge of the hole. These visible fretting zones are eroded oxidised black zones, so the boundary between fretting and non-fretting zones can be clearly distinguished. The width of these particles is up to 0.3 mm from the edge of the hole. Particles concentrated most against the load direction, and three-body fretting occurred in the fretting areas of the plate. Three-body fretting zones appear in black and contain deposits. Three-body fretting occurred at 480 N at 6×10^4 cycles. B contact surface wear scar width can be seen in Fig. 3. The wear scar width increased with cycle at 480 N.
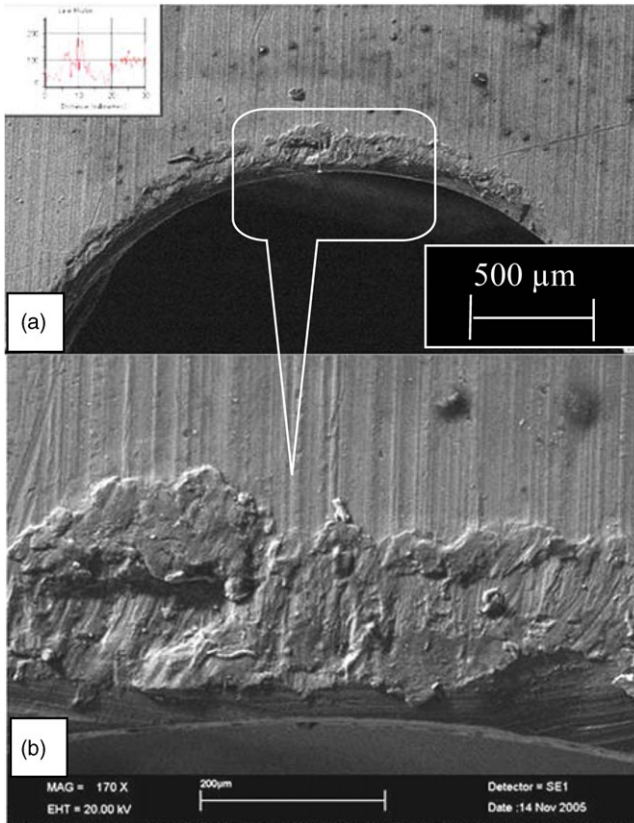
Figure 2. *Image of lower plate contact surface with rivet head (load: 480 N, cycle: 6×10⁴).*
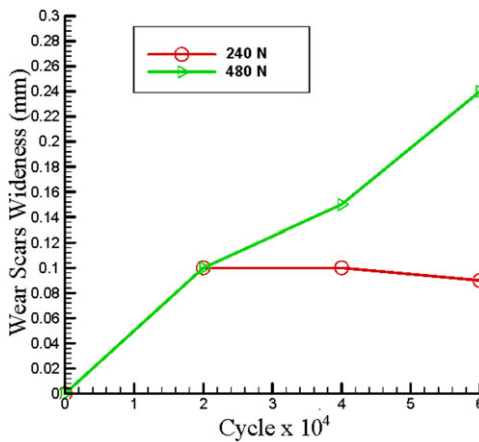

Figure 3. *Variation of wear scar width with cycle.*

4.0 Variation of surface roughness in fretting wear

Surface roughness is also important when friction and contact mechanisms are used to transmit power. Since the surface roughness has a great effect on the performance of the machine elements, the roughness changes during operation should be known.
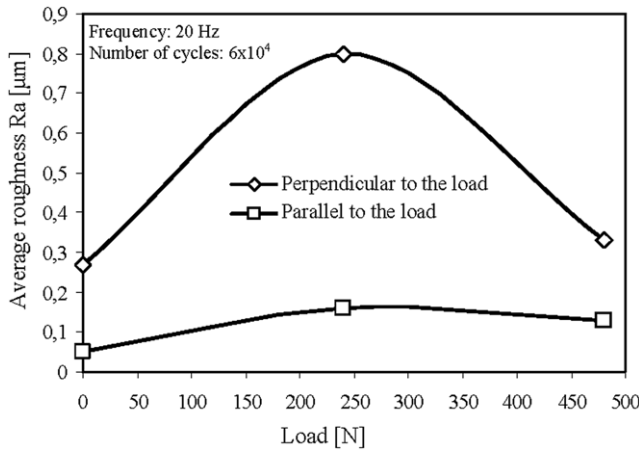
Figure 4. *Variation of rivet head contact surface roughness of upper plate with load.*

The roughness values of the plate surfaces in the joint areas were measured using the Mitutoyo Surftest 201 device. The average surface roughness Ra was tested using Mitutoyo 201 portable surface roughness tester. Measurements were made from the rivet head contact surface of the upper plate, the contact surface of the upper plate with the lower plate, the contact surface of the lower plate with the upper plate, and the rivet head contact surface of the lower plate. These surfaces are the parts shown in Fig. 1 as interface A, and interface B, respectively.

4.1. Effect of fretting damage on surface roughness
4.1.1 Variation of surface roughness with load

a) **Investigation of the Change of Surface Roughness of the Upper Plate with Load**

The reason for the high initial values in the measurements made perpendicular to the load is in terms of manufacturing. In the riveting process, the load direction and the manufacturing direction should be the same. The roughness values taken perpendicular to the manufacturing direction are higher than the values taken parallel to the manufacturing direction.

The variation of the mean roughness values measured on the upper plate in 6×10^4 cycles with the load is shown in Fig. 4. The roughness values measured perpendicular to the load were higher at 240 N.

The roughness values in 2×10^4 cycles measured perpendicular to the load were higher at 240 N. When higher loads are applied, the surface roughness is reduced due to the friction of the plates against each other. Surface roughness perpendicular to the load and parallel to the load became equal.

The average roughness values in 4×10^4 cycles was observed that the roughness decreased at 240 N and the roughness values increased at 480 N. Fretting scars began to appear when the cycle increased at 480 N, and the roughness values increased at 480 N due to increasing fretting scars. This is the transition phase from two-body fretting to three-body fretting. This is the stage where small residues begin to form. The variation of the mean roughness values measured at the interface between the upper plate and the lower plate in 6×10^4 cycles with the load is shown in Fig. 5. Since the cycle is high, it is seen that the roughness values increase at 240 N and 480 N (Fig. 5).

b) **Investigation of Lower Plate Surface Roughness Variation with Load**

The mean roughness values were measured at the interface between the lower plate and the upper plate in 2×10^4, 4×10^4 and 6×10^4 cycles. As with the upper plate, it was observed that the roughness values increased both at 240 N and 480 N due to the high cycle.
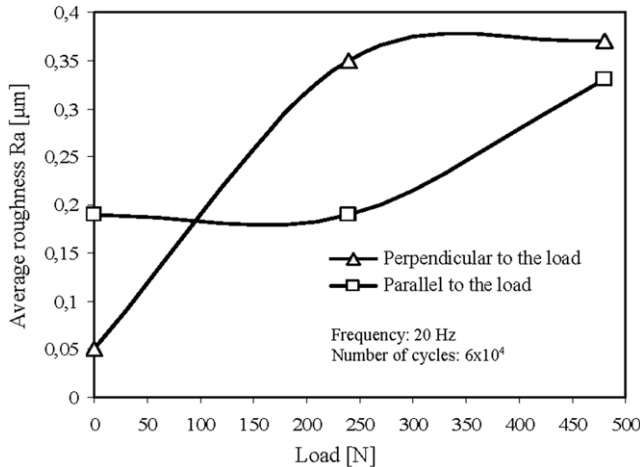
Figure 5. *Variation of the contact surface roughness of the upper plate with the lower plate with load.*

The mean roughness values were measured at the interface between the lower plate and the rivet head in 2×10^4, 4×10^4 and 6×10^4 cycles. The roughness values measured on the lower plate in 2×10^4 cycles decreased as the load increased. Only the roughness value perpendicular to the load increased as the load increased. The values measured at 4×10^4 cycles were greater at 480 N than at 240 N. According to the 6×10^4 cycle, the roughness values measured perpendicular to the load were higher at 240 N.

4.1.2 Investigation of the variation of surface roughness with cycling

When the roughness of the contact surface of the upper plate with the rivet head is examined with the cycle, it is seen that the roughness increases at 240 N and then decreases at 480 N, in the measurements made parallel to the load. In the direction perpendicular to the load, at 240 N, the roughness first increased, then decreased slightly, and when the 6×10^4 cycle was reached, the roughness increased due to fretting residues formed on the surface. At 480 N, on the other hand, the roughness value first increased and then decreased as the cycle was increased. Since the load is large at 480 N, the roughness of the manufacturing scars first increased, and when the cycle was increased, the surface roughness of the part decreased due to friction.

The variation of the roughness of the contact surface of the upper plate and the lower plate with the cycle is given in Fig. 6. When Fig. 6 is examined, it is seen that the roughness decreases slightly as the cycle increases due to the friction of the two plates in the measurements made parallel to the load. In the direction perpendicular to the load, the roughness first decreased due to the reduction in manufacturing traces with the effect of friction, and when the cycle was increased, the roughness increased due to the fretting resudues formed on the surface, especially at 480 N.

The variation of the contact surface roughness of the lower plate with the upper plate was also measured. In the measurements made parallel to the load, it is seen that the roughness decreases slightly as the cycle increases due to the friction of the two plates. In the direction perpendicular to the load, the roughness increased when the cycle was applied, and the roughness decreased and increased again as the cycle was increased. These changes are due to manufacturing direction and fretting residues.

When the changes in the contact surface roughness of the lower plate with the rivet head are examined, it is seen that the roughness increases at 480 N and then decreases at 240 N, in the measurements made parallel to the load. In the measurements made in the direction perpendicular to the load, the roughness increased with the effect of friction as the cycle increased.
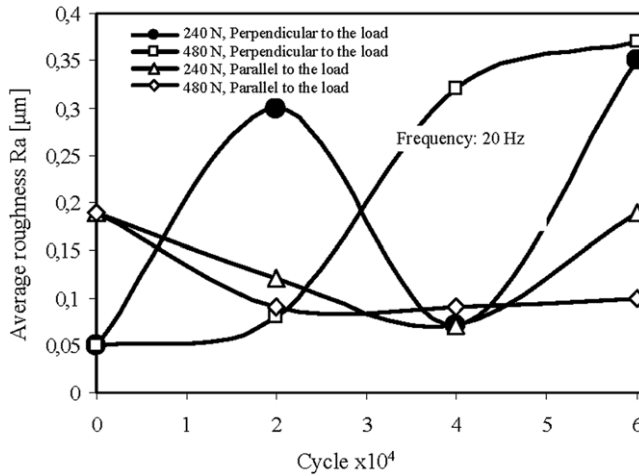
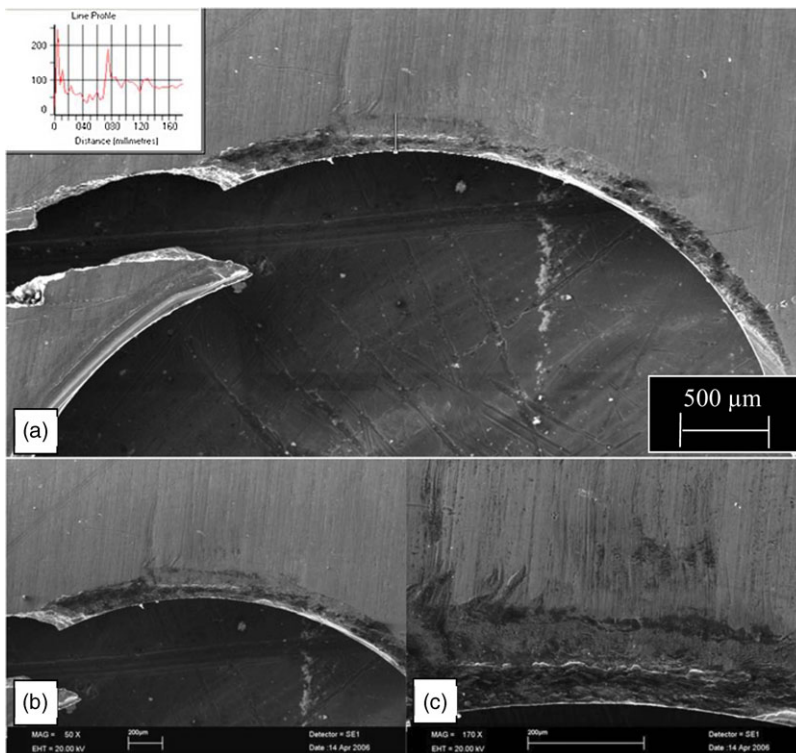**Figure 6.** *Variation of the contact surface roughness of the upper plate with the lower plate with cycling.*

Figure 7. *Lower plate contact surface with rivet head (load: 480 N, cycle: 866,920).*

5.0 Investigation of plate surfaces for the 866,920 fatigue cycle

Small residual particles were seen at the hole edge of the contact surface of the lower plate with the upper plate. These visible wear areas are worn oxidised black areas. Residues generally occurred in the cracked part of the bottom plate. First, cracks in the bottom plate were seen at 476,711 cycles (Fig. 7).
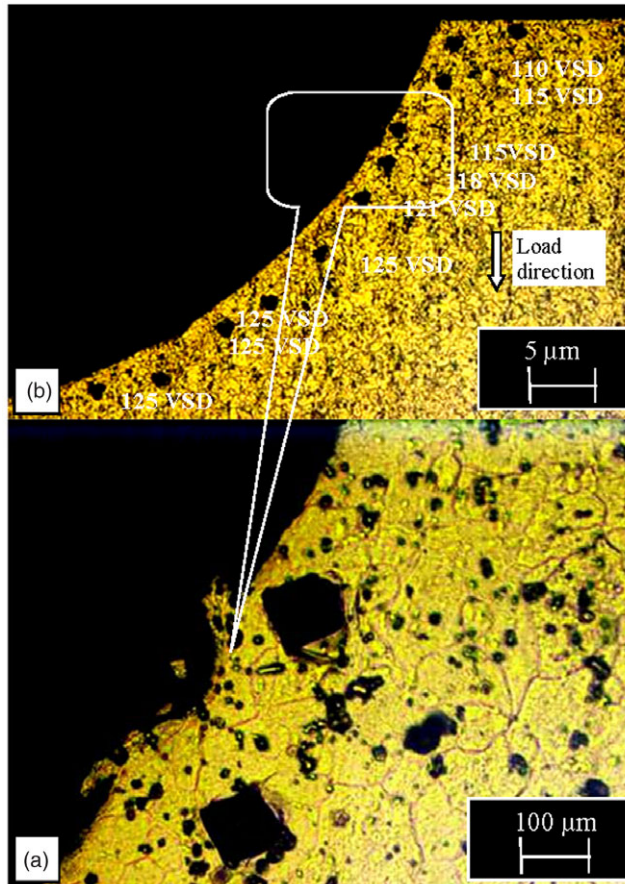
Figure 8. *a) Microhardness distribution of upper plate a contact surface with lower plate b) detail view (load: 480 N, number of cycles: 6×10^4).*

6.0 Change of microhardness in fretting wear

The microhardness distribution of the plates forming the rivet connection section and the rivet were determined with the mhp 160 model microhardness apparatus, which can be mounted on a Janevert brand metal microscope. In the microhardness measurements made on the rivet head and A contact surface of the upper plate in the rivet connection without the fretting test, it was determined that the average hardness of the hole circumference was 118 Vickers hardness value (VSD) and 113 VSD in the inside of the hole direction. As it can be understood from here, the hole edges have hardened due to the hardening during riveting.

In the rivet joint with 480 N and 6×10^4 cycles, it was determined that the microhardness of the contact surface of the upper plate with the lower plate A increased with fretting wear and reached an average of 122 VSD (Fig. 8).

It is seen in Fig. 9 that the rivet body is softer than the plate, according to the hardness distribution of the rivet and upper plate, which is not subjected to load testing.

The change graph of the hardness value scanned from the part of the rivet hole perpendicular to the load to the part parallel to the load is given in Fig. 10. The stiffness increased slightly as we approached the part of the hole perpendicular to the load. The hardness has increased since the load is forging in the part where the load comes vertically.
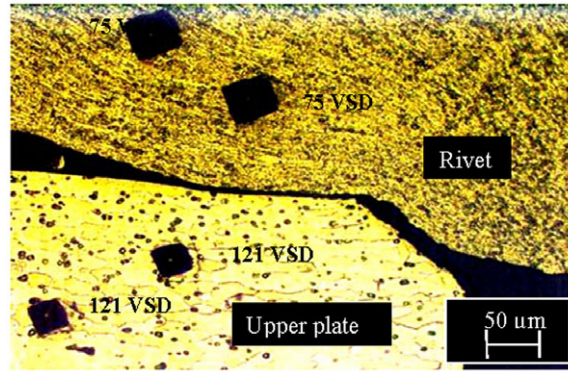
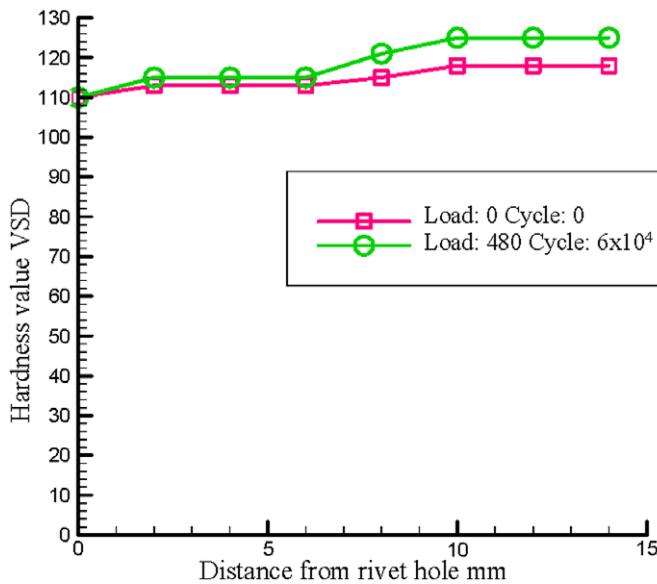**Figure 9.** *Microhardness distribution of upper plate contact surface with rivet head (load: 480 N, number of cycles: 6×10^4).*

Figure 10. *Comparison of microhardness values of loaded and unloaded plates.*

7.0 Metallographic examination

Metallographic examination was carried out in the joint areas of the samples. The joints were mounted to sand off the residue on the samples. It was then sanded with P1200 water sander. Polished surfaces are etched with keller etching. Thus, the grain structures were made visible. There was a change in the grain structures on the contact surfaces. Figures 11 and 12 show the grain structures of the cracked joint. Crack progression is clearly seen in the detail picture in Fig. 12. The crack propagates both from the grain boundary and over the grain.

Alloy 6,061 of nominal composition contains 1.0% Mg2Si, which melts in aluminium at 500°C. A higher amount of Mg2Si than this ratio reduces the solubility feature due to the excessive amount of magnesium. Silicon more than the amount to form Mg2Si and iron at normal levels decrease the melting of Mg2Si slightly.
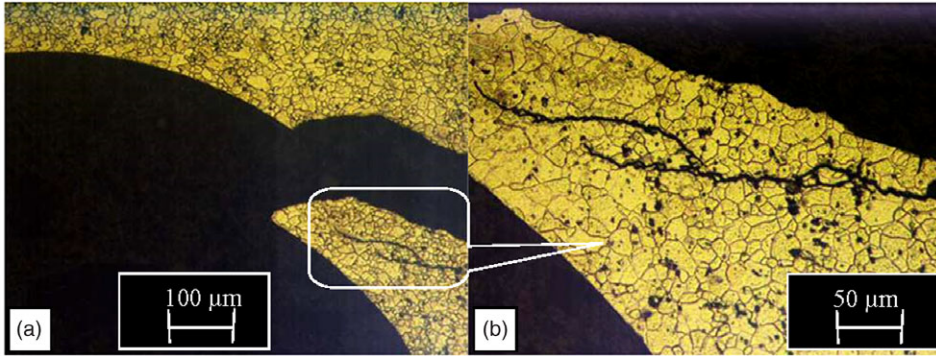
Figure 11. *a) Image of lower plate with upper plate contact surface crack. b) Detail image (load: 480 n, cycle: 866,920).*
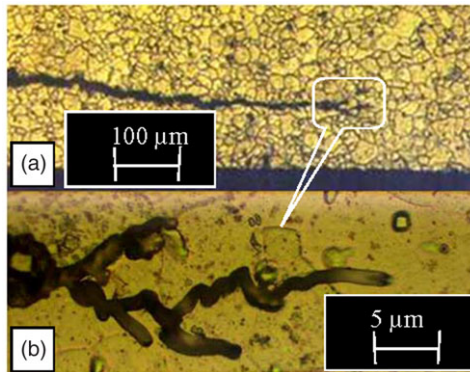

Figure 12. *a) Image of lower plate with upper plate contact surface crack. b) Detail image (load: 480 n, cycle: 866,920).*

When the alloy drops to a temperature below the solidus curve, Mg2Si precipitates. The amount and size of the precipitated particles depend on time and temperature. If slow cooling is made from the upper temperatures, large particles precipitate. Sudden cooling from above the solidus temperature to room temperature causes the magnesium and silicon to remain in solution, resulting in a supersaturated solid solution. In other words, the appropriate time should be waited at the specified temperature. In industrial plants, on the other hand, equilibrium situation rarely occurs. The solubility of Mg2Si in aluminium varies depending on the composition of the alloy and the rate of heating/cooling in the applied temperature range. As the re-solubility of Mg2Si is delayed above the solvus temperature, its dissolution under the solvus may also be delayed.

8.0 Conclusions

1. Fretting wear initially begins with metal-to-metal contact. Then, the formed metallic wear particles are hardened by oxidation. These hard particles spread between surfaces, causing three-body fretting wear.
2. Fretting wear surface width increases with increasing load and number of cycles.

3. The average width of fretting wear scar was 0.20 mm on the contact surface of the lower plate with the upper plate, and 0.119 mm on the contact surface of the lower plate with the rivet head.

4. The areas of least wear are the contact surface of the bottom plate with the rivet swelling head.

5. Average surface roughness changed with fretting wear. The mean surface roughness also increased with the increase in load. With the increase in the number of cycles, the average roughness of the surfaces with fretting wear also increased.

6. The fatigue life of the blind rivet joint was determined as 866,920 cycles. Fatigue rupture developed in the direction perpendicular to the load direction. Fatigue rupture occurred as grain and grain boundary rupture and developed as ductile + brittle rupture.

7. In the microhardness measurements made on the contact surface of the top plate with the rivet head in the rivet connection without the fretting test, it was determined that the average hardness of the hole circumference was 118 VSD and 113 VSD in the inside of the hole direction. Hole edges hardened during riveting.

8. Fretting wear increased with the microhardness of the contact surface of the upper plate and the lower plate, and it was determined to be an average of 122 VSD.

9. It was determined that a small amount of plastic deformation occurred in the contact areas of the rivet joint. In regions where plastic deformation is effective, the grains of the material tend to elongate by flowing in the direction of deformation.

References

[1] Kolanu, N.R., Raju, G. and Ramji, M. Damage assessment studies in CFRP composite laminate with cut-out subjected to in-plane shear loading, *Compos. Part B Eng.*, 2019, **166**, pp 257–271. https://doi.org/10.1016/j.compositesb.2018.11.142

[2] Thoppul, S.D., Finegan, J. and Gibson, R.F. Mechanics of mechanically fastened joints in polymer-matrix composite structures: a review, *Compos. Sci. Technol.*, 2009, **69**, pp 301–329. https://doi.org/10.1016/j.compscitech.2008.09.037

[3] Walker, P.B. Fretting in the light of aircraft experience, *J. R. Aeronaut. Soc.*, 1959, **63**, pp 293–298. https://doi.org/10.1017/s000192400009271x

[4] Gasson, P.C. Riveted lap joints in aircraft fuselage: Design, analysis and properties, *Aeronaut. J.*, 2014, **118**, pp 979–981. https://doi.org/10.1017/S0001924000009672

[5] Oskouei, R.H., Keikhosravy, M. and Soutis, C. A finite element stress analysis of aircraft bolted joints loaded in tension, *Aeronaut. J.*, 2010, **114**, pp 315–320. https://doi.org/10.1017/S0001924000003766

[6] Flower, H.M. and Soutis, C. Materials for airframes, *Aeronaut. J.*, 2003, **107**, pp 331–342. https://doi.org/10.1017/s0001924000013658

[7] Erena, D., Martín, V., Vázquez, J. and Navarro, C. Influence of the rolling of contact pads on crack initiation in fretting fatigue tests, *Int. J. Fatigue*, 2022, **163**, p 107087. https://doi.org/10.1016/j.ijfatigue.2022.107087

[8] Zhao, H., Xi, J., Zheng, K., Shi, Z., Lin, J., Nikbin, K., Duan, S. and Wang, B. A review on solid riveting techniques in aircraft assembling, 2020. https://doi.org/10.1051/mfreview/2020036

[9] Wang, J. and Zhou, C. Analysis of crack initiation location and its influencing factors of fretting fatigue in aluminum alloy components, *Chinese J. Aeronaut.*, 2022, **35**, pp 420–436. https://doi.org/10.1016/j.cja.2021.12.011

[10] Li, Z.Y., Liu, X.L., Wu, G.Q. and Huang, Z. Fretting fatigue behavior of Ti–6Al–4V and Ti–10V–2Fe–3Al alloys, *Met. Mater. Int.*, 2019, **25**, pp 64–70. https://doi.org/10.1007/S12540-018-0158-8/FIGURES/7

[11] Sadeler, R. and Öcal, M. Influence of relative slip on fretting fatigue behaviour of 2014 aluminium alloy with the age-hardened conditions T4 and T6, *Met. Mater. Int.*, 2012, **18**, pp 273–277. https://doi.org/10.1007/s12540-012-2010-x

[12] Dănăilă, E., Benea, L., Caron, N. and Raquet, O. Titanium carbide nanoparticles reinforcing nickel matrix for improving nanohardness and fretting wear properties in wet conditions, *Met. Mater. Int.*, 2016, **22**, pp 924–934. https://doi.org/10.1007/s12540-016-6090-x

[13] Sathish, M., Radhika, N. and Saleh, B. *Duplex and Composite Coatings: A Thematic Review on Thermal Spray Techniques and Applications*, Springer, 2022. https://doi.org/10.1007/s12540-022-01302-9

[14] Veillette, P.R. *Preventing Fretting Damage Becomes Increasingly Critical as Aircraft Age*, Flight Safety Foundation, 1998. https://flightsafety.org/amb/amb_nov-dec98.pdf

[15] Kragel′skiĭ, I.V. and Alisin, V.V. *Friction, Wear, Lubrication: Tribology Handbook*, Mir Publishers, 1981. https://www.abebooks.com/9780080275918/Friction-Wear-Lubrication-Tribology-Handbook-0080275915/plp

[16] Introduction Stol CH701 – Zenith Aircraft Company. https://zenithair.net/introduction-stol-ch701/

[17] Erarslan, Y. Etial-60 alaşımında döküm ve homojenizasyon uygulamalarının ekstrüzyon kabiliyetine etkileri, 1999. http://dspace.yildiz.edu.tr/xmlui/handle/1/1958

[18] Aircraft Construction, Riveted Joints (Part 2 of 2). http://www.zenithair.com/kit-data/ht-87-1.html

[19] Erturun, V. Uçaklardaki perçin bağlantılarında fretting yorulma ve aşınma davranışlarının incelenmesi, 2006. https://tez.yok.gov.tr/UlusalTezMerkezi/TezGoster?key=XohQ0H2mJnBfxLPsY8dG44f6rsCzJLoRPFCpURk0z1Otmq6HS3T_lyZ6QxXYpfM2